CI&CEQ
Chemical Industry & Chemical Engineering Quarterly

Available online at
Association of the Chemical Engineers of Serbia AChE
www.ache.org.rs/CICEQ

Chem. Ind. Chem. Eng. Q. 32 (3) 245–255 (2026) CI&CEQ

MEHMET SOYDAN
İBRAHIM DOYMAZ

Yildiz Technical University,
Department of Chemical Engineering
İstanbul, Türkiyea

INFRARED DRYING OF CARROT SLICES: EFFECT OF POWER LEVELS ON KINETICS AND ENERGY EFFICIENCY

Highlights

- The drying process of carrot slices using an infrared dryer was conducted.
- Drying time decreased with increasing infrared power level.
- The Midilli & Kucuk model better fits all the applied drying conditions.
- The highest effective moisture diffusivity was obtained in samples dried at an 88 W IR power level.

Abstract

The aim of this study is to optimize the drying conditions for yellow carrots by investigating the effects of varying infrared (IR) power levels on drying kinetics. Following drying tests at IR power levels of 38, 50, 62, 74, and 88 W, the initial moisture content of carrot slices (6.95 kg water/kg dry matter) was decreased to 0.11 kg water/kg dry matter. Drying times ranged from 300 minutes at 38 W to 110 minutes at 88 W, demonstrating an inverse relationship between IR power and drying duration. Higher IR power levels accelerated the drying rate by enhancing energy transfer, which promoted moisture removal efficiency. Effective diffusion coefficients, calculated as ranging from 7.73×10^{-10} to 2.21×10^{-9} m²/s for the power levels of 38 W to 88 W, indicate an increase in moisture migration with higher power. The process's energy requirements were reflected in the activation energy for moisture diffusion (1.967 kW/kg). The Midilli and Kucuk model offered the best fit for characterizing the drying behaviour, and statistical analysis validated the model's correctness. These findings provide valuable insights for optimizing IR drying conditions to enhance the efficiency and quality of yellow carrot drying processes.

Keywords: Infrared drying, mathematical modelling, drying kinetics, diffusion coefficient, activation energy.

SCIENTIFIC PAPER

UDC 633.43:66.047.3.085.1:519.87

INTRODUCTION

Carrots, cultivated worldwide for over two millennia, represent a versatile root vegetable characterized by variations in shape, size, and colour, with the orange type being predominant. Carrots, which have only 171.5 kJ per 100 grams, have several health benefits, such as preventing diabetes, heart disease, night blindness, cataracts, and some types of cancer [1]. Post-harvest decay remains a major obstacle to extending the shelf life of vegetables, with approximately 17% of total produce lost during post-harvest handling. Various preservation techniques are employed to mitigate this issue, including refrigeration and controlled atmosphere storage. While exposure to elevated temperatures can result in wilting and reduce the aesthetic quality of carrots, significant quantities are dried in many agricultural regions to improve durability, lower transportation weight, and maintain both flavour and nutritional integrity [2].

The primary method of heat transfer in drying operations is convection, which causes water to evaporate into the air as heat is transferred from hot air to the product. However, there are several drawbacks to convective drying of agricultural goods, mostly related to the indirect heating mechanism via air, such as long drying durations, variable product quality, low efficiency, and high energy requirements. Alternative drying methods have been developed because of these inefficiencies [3].

Infrared drying presents numerous advantages over traditional methods, including faster drying times, greater energy efficiency, uniform temperature distribution, superior product quality, improved process control, high heat transfer rates, spatial efficiency, and environmental sustainability. Recent advancements in radiator technology have enhanced its efficiency and compact design. The absorption of IR energy by water is critical to drying kinetics,

Correspondence: İ. Doymaz, Yildiz Technical University, Department of Chemical Engineering, 34220 Esenler, İstanbul, Türkiye.
Email: doymaz@yildiz.edu.tr
Paper received: 28 June 2025
Paper revised: 15 October 2025
Paper accepted: 19 November 2025

https://doi.org/10.2298/CICEQ250628028S

with moist, porous materials enabling deeper radiation penetration, which diminishes as moisture content reduces [4,5].

A precise method for describing drying kinetics, especially in agricultural products, is mathematical modelling. This approach relies on the application of correlation and regression statistical methods to formulate equations that accurately depict the dynamics of the drying process. Various experimental models have been extensively studied, particularly for the falling rate drying phase. Frequently utilized models include linear, power, exponential, Arrhenius, and logarithmic functions, with polynomial models applied when these alternatives yield low determination coefficients [6, 7].

This research seeks to establish a predictive model for moisture reduction in carrot drying, aligning quality parameters with the product's thermal and moisture behaviours to enhance process control precision. Mathematical modeling provides a cost-effective alternative for manufacturers, fostering innovation in product and process development while circumventing the high costs associated with experimental trials. The study is to simulate the infrared drying process for carrot slices, evaluate the drying process's energy efficiency at different IR power levels, and ascertain the activation energy needed for efficient moisture removal. The diffusion coefficient of sample drying was calculated, and a correlation between the mathematical models and moisture ratio, indicating water loss, was established. Statistical analysis was conducted to validate and verify the models. Additionally, the study intends to assess the effectiveness of infrared drying as a drying method with the dynamics of heat and mass transfer during the process of drying samples.

This study aims to develop a predictive model for moisture reduction during the infrared drying of carrot slices, integrating key quality parameters with the fundamental thermophysical and hydric behaviour of the product to achieve superior process control. A critical synthesis of the extant literature identified a pronounced research gap: although investigations into drying kinetics, quality degradation, and empirical modeling are plentiful, there is a conspicuous absence of systematic analysis concerning energy efficiency across a spectrum of infrared power densities. This work directly addresses this omission by conducting a concurrent investigation into the drying characteristics and energy consumption metrics of carrot slices under infrared radiation. The employment of mathematical modeling presents an economically viable strategy for industry, circumventing the prohibitive costs of extensive experimental trials and thereby accelerating innovation in both product and process development. Our methodology entails the determination of the effective moisture diffusivity and the activation energy requisite for efficient desorption. Furthermore, we established a rigorous correlation between theoretical models and the experimental moisture ratio to quantitatively describe the dehydration process. The validity of these models was ascertained through robust statistical verification. Ultimately, this research provided a holistic evaluation of infrared drying by synergistically examining energy efficiency, kinetic parameters, and the underlying heat and mass transfer phenomena. This integrated approach yields novel insights for the optimization of energy utilization without compromising drying efficacy, thereby contributing advanced and actionable knowledge to the field of food engineering and drying technology.

MATERIAL AND METHODS

Materials

Freshly harvested carrots (*Daucus carota* L. subsp. sativus) were obtained from the local market in Beypazarı (Türkiye). The samples were cut into uniform discs (6 ± 0.1 mm thickness, 40 ± 0.1 mm diameter). The initial moisture content, determined by the AOAC method [8], was 87.42% (wet basis).

Experimental procedure

A laboratory-scale infrared dryer (Snijders Moisture Balance, Snijders b.v., Tilburg, Holland) with a power range of 38 W to 88 W was used for the drying tests. Carrot slices were placed evenly and homogeneously across an aluminium tray, ensuring a uniform thin-layer distribution. A sample mass of 38±0.1 g, consisting of eight cylindrical carrot slices, was loaded in a single layer for each drying run. The drying process was carried out at varying infrared power levels, set through the equipment's control unit. Moisture loss was measured at 10-minute intervals with a digital balance (Mettler-Toledo AG, Greifensee, Switzerland, model BB3000), with an accuracy of 0.1 g. The drying was continued until the samples reached a final moisture content of 10% (wb). The carrot slices were dehydrated to a final moisture content of approximately 13–14% (wet basis), which is generally regarded as the optimal level for safe storage [9]. In the present study, however, a target moisture level of around 10% was selected to ensure the stability of the dried samples for subsequent analyses. Drying beyond this point was intentionally avoided for two primary reasons: energy efficiency and product quality preservation. Excessive drying below 10% would not only lead to unnecessary energy consumption but also increase the risk of quality degradation, as prolonged exposure to hot air can adversely affect both the texture and the nutritional properties of carrots. Moreover, as the moisture content decreases, the driving force for mass transfer between the carrot slices and the drying air diminishes, thereby extending drying time. This prolonged process can further exacerbate quality losses. In addition, the phenomenon of case hardening [10] - a condition where a hardened surface layer forms during drying – impedes effective moisture removal, making it more difficult to reduce the moisture content below 10%. For these reasons, maintaining the final moisture level at approximately 10% was considered both a practical and scientifically sound approach. After drying, the samples were cooled and sealed in low-density polyethylene (LDPE) bags for storage. To form the drying curves, the average moisture content was determined after each experiment was run in triplicate.

Mathematical modeling

Moisture content was computed with the equation:

$$M = \frac{M_w}{M_d} \quad (1)$$

where M_w is the sample's wet weight (kg), M_d is its dry weight (kg), and M is the moisture content (kg water/kg dry matter). The eleven thin-layer drying models displayed in Table 1 were fitted to the data gathered from the drying of carrot slices. Eq. (2) was used to determine the moisture ratio (MR) values from the designated models.

$$MR = \frac{M_t - M_e}{M_0 - M_e} \quad (2)$$

where M_t, M_0, and M_e are the moisture content at any time, the initial moisture content, and the equilibrium moisture content (kg water/kg dry matter), respectively, and t is the drying time (min). The values of M_e are minute relative to M_t and M_0 for a long drying period, so a simplified form of the moisture ratio can be used as expressed in Eq. (3):

$$MR = \frac{M_t}{M_0} \quad (3)$$

The drying rate *(DR)* of carrot slices was calculated using Eq. (4):

$$DR = \frac{M_t - M_{t+\Delta t}}{\Delta t} \quad (4)$$

where M_t and $M_{t+\Delta t}$ is moisture contents at t and $t+\Delta t$ (kg water/kg dry matter), respectively, and t is time (min).

Statistical analysis

To analyze the data, Statistica 10.0 (StatSoft Inc., Tulsa, OK, USA) was utilized. The model parameters were estimated using a non-linear regression technique, and the fit was maximized using the Levenberg-Marquardt technique. Three statistical criteria–the coefficient of determination (R^2), reduced chi-square (χ^2), and root mean square error (RMSE)–were used to evaluate how well the model fit the experimental data. These metrics were calculated using specific equations, providing a comprehensive evaluation of the models' predictive performance by measuring the goodness-of-fit and deviation of the predicted values from the observed data. The aforementioned parameters were computed using the mathematical expressions in Eqs. (5), (6), and (7). These formulas are designed to quantify the accuracy and reliability of the model predictions. As a measure of the model's explanatory capacity, the R^2 shows the percentage of variance in the observed data that can be explained by the model. The χ^2 assesses the goodness-of-fit by accounting for the degree of freedom, while the RMSE quantifies the average deviation between predicted and observed values, offering insight into the model's predictive precision [22].

$$R^2 = 1 - \frac{\sum_{i=1}^{N}(MR_{\exp,i} - M_{\text{pre},i})^2}{\sum_{i=1}^{N}(MR_{\text{pre}} - MR_{\exp,i})^2} \quad (5)$$

$$x^2 = \frac{\sum_{i=1}^{N}(MR_{exp,i} - MR_{\text{pre},i})^2}{N-n} \quad (6)$$

$$RMSE = \left[\frac{1}{N}\sum_{i=1}^{N}\left(MR_{\text{pre},i} - MR_{\exp,i}\right)^2\right]^{\frac{1}{2}} \quad (7)$$

The experimentally observed and model-predicted moisture ratio values are denoted by MR_{exp} and MR_{pre}, respectively, in these equations. N refers to the number of parameters, whereas n indicates the total number of experimental data points. The model with the lowest values of RMSE and χ^2; the highest R^2-value indicated the best fit for explaining the drying behaviour of the samples [23].

Assessment of effective moisture diffusivity

Internal diffusion processes primarily regulate the moisture transfer during the lowering rate stage, which is when the drying process usually takes place. Fick's second rule of unsteady-state diffusion is widely used to characterize the drying kinetics in this phase for a range of materials. This equation provides a mathematical framework that links the concentration gradient of moisture within the material to the rate of diffusion, allowing a comprehensive understanding of how moisture transfers from the interior to the surface during drying. By utilizing Fick's second law, researchers can effectively model and predict the dynamics of moisture removal, facilitating the optimization of drying processes and improving the quality of the final product [24]:

$$\frac{\partial M}{\partial t} = \nabla\left(D_{\text{eff}}\nabla M\right) \quad (8)$$

When Crank [25] solved the diffusion equation (Eq. 8) for the slab geometry, it was assumed that the initial moisture distribution was uniform, with low external resistance, constant diffusion, and minimal shrinkage:

$$MR = \frac{8}{\pi^2}\sum_{n=0}^{\infty}\frac{1}{(2n+1)^2}\exp\left(-\frac{(2n+1)^2\pi^2 D_{\text{eff}}t}{4L^2}\right) \quad (9)$$

where n is a positive integer, L is the slab's half-thickness in samples (m), and D_{eff} is the effective moisture diffusivity (m^2/s).

Eq. (9) can be simplified to get an approximate but reasonable prediction of drying kinetics during the early phases of the decreasing rate period when carrot drying is viewed as an infinite slab geometry. Only the series' dominating term is considered in this simplification, which is predicated on lengthy drying times. When characterizing the behaviour of moisture diffusion during prolonged drying periods, this reduction offers a compromise between computing efficiency and allowable inaccuracy [26]. The approximate analytical solution of Eq. (9) for slab shape is provided in Eq. (10) below, assuming a uniform starting moisture distribution, negligible external mass transfer resistance, and minimum shrinkage.

$$MR = \frac{8}{\pi^2}\exp\left(-\frac{\pi^2 D_{\text{eff}}t}{4L^2}\right) \quad (10)$$

Slope from Eq. (11) is used to determine effective moisture diffusivity. A linear relationship with a slope represented by K is obtained when the natural logarithm of the moisture ratio (MR) is plotted versus time. From this, Eq. (11) is derived, allowing for a precise estimation of effective moisture diffusivity. This approach provides a robust method for analysing the drying kinetics, as the linearity in the plot reflects the diffusion-controlled nature of

the moisture removal process, further enabling the accurate quantification of diffusivity [27]:

$$K = \frac{\pi^2 D_{\text{eff}}}{4L^2} \quad (11)$$

Calculation of the activation energy

A modified form of the Arrhenius equation was applied to describe the relationship between effective diffusivity and the ratio of infrared power to sample weight. This approach allows for the calculation of activation energy, which was determined using Eq. (12). The adapted model provides valuable insight into how varying infrared power levels influence the moisture removal process, enabling more precise control and optimization of drying conditions to improve efficiency and product quality [28].

$$D_{\text{eff}} = D_0 \exp\left(-\frac{E_a m}{P}\right) \quad (12)$$

In this equation, D_0 denotes the pre-exponential factor (m²/s), E_a is the activation energy (W/kg), P is the infrared power (W), and m is the sample weight (kg), collectively governing the dependence of effective moisture diffusivity on power input.

Efficiency of drying process

Drying efficiency measures the effectiveness of energy utilization in the moisture removal process during drying. It serves as a key indicator of the performance of drying systems, reflecting the equilibrium between energy consumption and the rate of moisture evaporation. High drying efficiency suggests that a substantial portion of the input energy is efficiently used for moisture extraction, minimizing energy wastage. Several factors, including drying temperature, infrared power levels, air velocity, and the intrinsic properties of the material, significantly impact drying efficiency. Optimizing these variables is essential for enhancing process sustainability, reducing energy consumption, and lowering operational costs [29,30].

Infrared drying efficiency was calculated as the ratio of the total heat energy provided by the drying system to the thermal energy needed to remove the moisture from the carrot slices. This metric provides insight into how effectively the energy delivered by the dryer is harnessed for the intended purpose of moisture removal, offering a quantitative measure of energy utilization. A higher ratio indicates greater efficiency, signifying that a larger portion of the supplied heat is being effectively converted into latent heat for water evaporation, rather than being lost through other processes, such as heat dissipation to the surroundings [31].

$$\eta = \left(\frac{m_w \lambda_w}{P t}\right) \times 100 \quad (13)$$

In Eq. (13), η represents the infrared drying efficiency (%), where P is the applied infrared power (W), m_w is the mass of evaporated water (g), and t is the drying duration (min). The latent heat of vaporization of water (λ_w), taken as 2257 J/g, specifies the energy required for phase transition under isothermal conditions. This formulation provides a concise yet rigorous means of quantifying the proportion of infrared energy effectively utilized for moisture removal, offering a robust basis for evaluating energy efficiency, optimizing process parameters, and advancing sustainable drying technologies [28].

RESULTS AND DISCUSSION

Drying curves

Drying behavior of carrot slices under the infrared method at varying power levels, as depicted in Fig. 1, demonstrates that moisture removal rates increase with rising infrared power. This is due to a greater moisture concentration gradient within the carrot slices, accelerating moisture diffusion. The higher power densities of the halogen lamp of the infrared dryer, such as 88 W, significantly reduce the drying time.

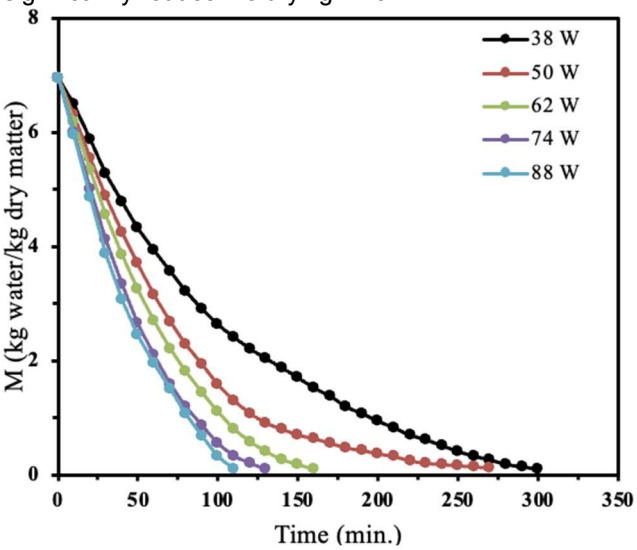

Figure 1. Carrot slice drying curves at different levels of infrared power.

Since larger energy rates are applied to the material, which results in the enlargement of both intracellular and intercellular pores in the carrot tissue, increased infrared power levels enable a quick decrease in the moisture content of the carrot. This structural change enhances water vapour diffusion from the carrot slices to the surrounding environment, thus lowering drying time. Such observations align with prior studies, including carrot [32], apple [33], and lemon slices [34]. In these studies, high drying intensities promoted structural cracking and shortened the overall processing time by improving water diffusion.

Fig. 2 shows the drying rate curves for carrot slices, where no drying period at a constant rate was observed for all experimental conditions, indicating that the drying process occurred after a short preheating period with a completely falling-rate period. This behaviour highlights diffusion as the main mechanism controlling moisture transport in carrot slices by showing a consistent drop in moisture content over the course of the drying period. This is in agreement with previously published studies on root vegetables, which emphasize that moisture removal during IR drying is predominantly governed by internal moisture diffusion rather than surface evaporation [2]. Furthermore, an increase in infrared power led to an elevated drying rate, signifying that higher infrared power enhances both heat and mass transfer, thereby accelerating water loss from the

samples.

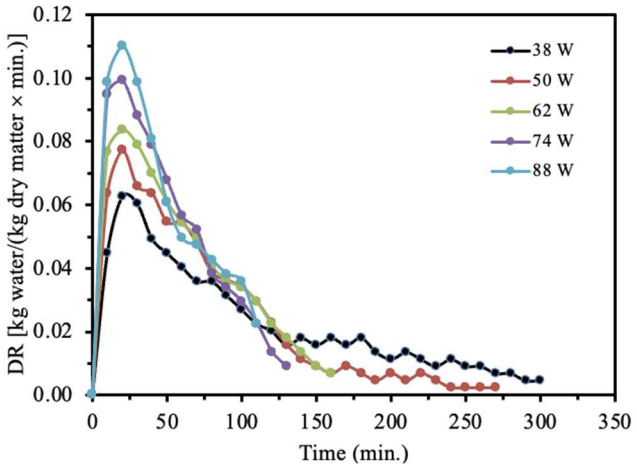

Figure 2. Carrot slice drying rate curves with respect to drying time for different IR power levels.

Initial drying rates were higher during the drying process, but they gradually decreased as the moisture content declined. This reduction in drying rate is likely due to the decreased porosity of the samples, resulting from shrinkage over time, which heightens resistance to water migration and further slows the drying rate. This shrinkage effect has been well documented in convective and infrared drying studies, where tissue densification narrows capillary pathways and lowers effective moisture diffusivity. These findings align well with prior research on drying kinetics in agricultural materials [35-37]. These studies similarly identified a falling-rate period in the drying process, attributed to structural transformations within the material that reduce moisture diffusivity. Such structural changes can hinder moisture migration pathways, thus decelerating the drying rate. This phase underscores the importance of internal structural shifts, which profoundly impact moisture retention, drying efficiency, and overall product quality throughout the drying cycle.

Modelling of thin-layer drying processes for carrot slices

The drying experiments' moisture content data were transformed into moisture ratio (MR) values, as indicated in Table 1, and these values were then applied to fit various thin-layer drying models. Eleven distinct models were evaluated to determine which one would be best for forecasting sample drying times. To assess model accuracy, statistical indices, including the R^2, the χ^2, and *RMSE*, were calculated to measure the goodness of fit, as presented in Eqs. (4), (5), and (6). The selection criterion for the optimal model was based on the highest R^2 value combined with the lowest χ^2 and *RMSE* values. For the range of experiments, the models yielded R^2 values between 0.988 and 1.000, *RMSE* values from 0.0033 to 0.0507, and χ^2 values ranging from 0.0014 to 0.3114. These statistical outputs provided insight into the precision and predictive accuracy of each model.

Table 2 presents the parameter estimates for eleven mathematical models applied to carrot slices, reflecting variations attributable to different infrared power levels. Each parameter estimate achieved statistical significance, meeting or exceeding a 1% significance level, thereby demonstrating the models' robustness and precision in characterizing drying kinetics under diverse experimental conditions. Notably, the Midilli & Kucuk model exhibited superior performance relative to the other models, as evidenced by its highest R^2 and lowest values for χ^2 and RMSE, indicating its exceptional fit and reliability in accurately modelling the drying behaviour.

Table 1. Semi-empirical models utilized in the analysis of carrot slice drying.

Name of Model	Model	Reference
Lewis	$MR = \exp(-kt)$	[11]
Henderson and Pabis	$MR = a\exp(-kt)$	[12]
Logarithmic	$MR = a\exp(-kt) + c$	[13]
Midilli and Kucuk	$MR = a\exp(-kt^n) + b$	[14]
Wang and Singh	$MR = 1 + at + bt^2$	[15]
Aghbashlo *et al.*	$MR = \exp\left(-\frac{at}{1+bt}\right)$	[16]
Page	$MR = \exp(-kt^n)$	[17]
Logistic	$MR = \frac{b}{1 + a\exp(-kt)}$	[18]
Jena and Das	$MR = a\exp\left(-kt + b\sqrt{t}\right) + c$	[19]
Vega-Galvez I	$MR = \exp(n + kt)$	[20]
Vega and Lemus	$MR = (a + kt)^2$	[21]

The validity of the selected model for carrot slices dried at various infrared power levels is confirmed by comparing experimental moisture ratios (*MR*) with those predicted by the Midilli & Kucuk model in Fig. 3. Because the data points are precisely aligned along a 45° line, the findings show a significant agreement between the experimental and projected *MR* values, confirming the model's appli-cability for drying behavior of samples.

Effective moisture diffusivity

Plotting the logarithm of the moisture ratio (MR) regarding drying time at various infrared power levels was done using the experimental data. The effective moisture diffusivity (D_{eff}) values for each infrared power level, computed by Eq. (11), are shown in Fig. 4. A power level of 38 W produced the lowest D_{eff} and a power level of 88 W produced the highest D_{eff}. These findings indicate that higher power levels promote more effective drying of carrot slices within the studied parameters. This is attributed to the relatively high D_{eff} values obtained, which suggest enhanced moisture mobility within the samples. When the power level rose, the impact on the D_{eff} became significantly more apparent compared to lower power levels, as illustrated distinctly in Fig. 4. This effect can be attributed to the rapid temperature increase in carrot slices under high infrared power, which raises the vapour pressure and, in turn, accelerates the drying rate.

Table 2 Assessment of infrared-dried carrot slices at varying power levels using statistical metrics for thin-layer drying models.

IR power	Model	Model Constants					R^2	χ^2	RMSE
		a	*b*	*c*	*k*	*n*			
38	Lewis				0.0119		0.9928	0.2123	0.0363
	Henderson & Pabis	1.0803			0.0128		0.9959	0.1156	0.0231
	Logarithmic	1.1049		-0.0451	0.0113		0.9975	0.3114	0.0181
	Midilli & Kucuk	0.9978	0.0002		0.0032	1.2819	0.9997	0.0095	0.0062
	Wang & Singh	-0.0084	0.0001				0.9968	0.0957	0.0240
	Aghbashlo *et al.*	0.0092	-0.0019				0.9988	0.0110	0.0146
	Page				0.0036	1.2590	0.9996	0.0379	0.0069
	Logistic	1.7968	0.7754		0.0183		0.9995	0.0328	0.0067
	Jena & Das	-0.0905	0.3226	1.1341	0.0103		0.9982	0.1377	0.0162
	Vega-Galvez I				-0.0128	0.0773	0.9959	0.1156	0.0231
	Vega & Lemus	0.9941	-0.0041				0.9969	0.0844	0.0226
50	Lewis				0.0142		0.9957	0.1071	0.0274
	Henderson & Pabis	1.0572			0.0150		0.9973	0.0601	0.0187
	Logarithmic	1.0714		-0.0272	0.0139		0.9980	0.1681	0.0163
	Midilli & Kucuk	0.9921	0.0004		0.0050	1.2353	0.9998	0.0059	0.0050
	Wang & Singh	-0.0098	0.0002				0.9933	0.4931	0.0326
	Aghbashlo *et al.*	0.0118	-0.0017				0.9990	0.0889	0.0118
	Page				0.0060	1.1934	0.9997	0.0514	0.0070
	Logistic	2.0568	1.0470		0.0202		0.9997	0.0527	0.0064
	Jena & Das	-0.1197	0.3082	1.1565	0.0105		0.9979	0.1624	0.0176
	Vega-Galvez I				-0.0150	0.0556	0.9973	0.0601	0.0187
	Vega & Lemus	0.9775	-0.0046				0.9948	0.0734	0.0283
62	Lewis				0.0187		0.9904	0.1842	0.0434
	Henderson & Pabis	1.0724			0.0200		0.9934	0.1271	0.0360
	Logarithmic	1.1481		-0.1068	0.0156		0.9978	0.1292	0.0207
	Midilli & Kucuk	0.9949	-0.0006		0.0053	1.2996	0.9999	0.0014	0.0031
	Wang & Singh	-0.0137	0.0004				0.9993	0.0303	0.0113
	Aghbashlo *et al.*	0.0137	-0.0037				0.9994	0.0590	0.0103
	Page				0.0051	1.3114	0.9998	0.0034	0.0053
	Logistic	1.5462	0.5451		0.0316		0.9998	0.0036	0.0039
	Jena & Das	-0.0512	0.5049	1.0684	0.0211		0.9992	0.0253	0.0119
	Vega-Galvez I				-0.0200	0.0699	0.9934	0.1271	0.0360
	Vega & Lemus	1.0025	-0.0068				0.9987	0.0907	0.0137
74	Lewis				0.0204		0.9915	0.1447	0.0405
	Henderson & Pabis	1.0567			0.0216		0.9937	0.1117	0.0350
	Logarithmic	1.1788		-0.1578	0.0155		0.9993	0.0085	0.0111
	Midilli & Kucuk	0.9976	-0.0003		0.0089	1.1837	0.9999	0.0029	0.0033
	Wang & Singh	-0.0151	0.0005				0.9997	0.0084	0.0064
	Aghbashlo *et al.*	0.0153	-0.0038				0.9998	0.0010	0.0037
	Page				0.0069	1.2692	0.9993	0.0221	0.0114
	Logistic	1.6152	0.6245		0.0331		0.9995	0.0169	0.0089
	Jena & Das	-0.0555	0.5099	1.0655	0.0222		0.9996	0.0075	0.0086
	Vega-Galvez I				-0.0216	0.0551	0.9937	0.1117	0.0350
	Vega & Lemus	0.9957	-0.0073				0.9992	0.1405	0.0118
88	Lewis				0.0234		0.9876	0.1690	0.0507
	Henderson & Pabis	1.0668			0.0249		0.9905	0.1302	0.0442
	Logarithmic	1.2354		-0.2073	0.0166		0.9984	0.0146	0.0174
	Midilli & Kucuk	0.9961	-0.0003		0.0072	1.2816	0.9998	0.0037	0.0051
	Wang & Singh	-0.0172	0.0007				0.9995	0.0044	0.0093
	Aghbashlo *et al.*	0.0163	-0.0054				0.9997	0.0052	0.0067
	Page				0.0058	1.3560	0.9993	0.0167	0.0113
	Logistic	1.4242	0.4316		0.0422		0.9996	0.0124	0.0082
	Jena & Das	-0.0375	0.6307	1.0448	0.0301		0.9997	0.0079	0.0076
	Vega-Galvez I				-0.0249	0.0647	0.9905	0.1302	0.0442
	Vega & Lemus	1.0049	-0.0086				0.9995	0.0574	0.0095

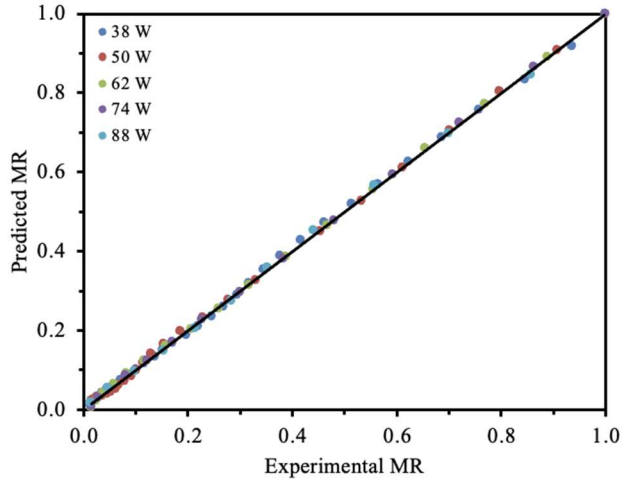

Figure 3. Carrot slice moisture ratios, both experimental and anticipated, at different IR power levels using the Midilli & Kucuk model

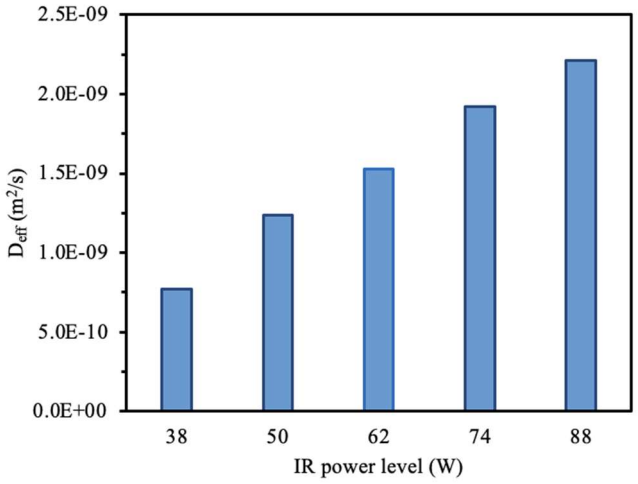

Figure 4. Effect of infrared power levels on effective diffusion coefficient.

The D_{eff} values in this study ranged from 7.73×10^{-10} to 2.21×10^{-9} m²/s, which aligns with those reported for other drying methods and agricultural products. For instance, in laboratory-scale convective drying of peach slices, D_{eff} values were reported to range from 9.57×10^{-10} to 4.33×10^{-9} m²/s across a temperature spectrum of 40-80°C [38]. In a similar context, the drying of okra yielded D_{eff} values between 2.89×10^{-9} and 12.23×10^{-9} m²/s at radiation intensities of 0.167, 0.235, and 0.520 W/cm² [39]. These comparable values reinforce the reliability of our experimental data and confirm that the observed diffusivities are within the expected range for plant-based tissues under IR drying.

To provide a prediction model for comprehending D_{eff} dynamics under various drying conditions, a multiple regression analysis was also performed to explain the relationship between moisture diffusivity and power level. The correlation between the infrared power range utilized in our experimental studies and effective moisture diffusivity is articulated through the following equation:

$$D_{eff} = 2.86\times10^{-11}P - 2.43\times10^{-10}$$
$$R^2 = 0.988 \qquad (14)$$

where P represents the power level, measured in watts (W). This equation can serve as a practical predictive tool for estimating moisture transport rates in similar food matrices under IR drying conditions, thereby assisting in the design of energy-efficient drying protocols.

Activation energy

According to Eq. (12), the activation energy (E_a) was determined by plotting ln (D_{eff}) against m/P (sample weight/infrared power in kg/W), which is the slope of the Arrhenius equation. Fig. 5 illustrates the relationship between ln (D_{eff}) and m/P. The slope of the line in Fig. 5 represents ($-E_a$), while the intercept corresponds to ln (D_0). According to these findings, the Arrhenius dependence is supported by a linear connection. The impact of the sample weight-to-power ratio on D_{eff} is captured by Eq. (15), with coefficients defining this relationship:

$$D_{eff} = 4.86\times10^{-9}\exp\left(-\frac{1967.5\ m}{P}\right)$$
$$R^2 = 0.999 \qquad (15)$$

The maximal diffusion coefficients (D_0) at infinite temperature and the activation energy (E_a) for carrot samples were derived using a modified Arrhenius-type exponential model, as indicated by Eq. (15). These parameters provide insights into the diffusion behaviours and thermal activation characteristics across the different samples. Specifically, the highest diffusivity that any sample may have under idealized thermal conditions is indicated by the theoretical diffusion coefficient at infinite temperature, or D_0. In contrast, E_a quantifies the minimum energy barrier required for diffusion to occur, reflecting the sensitivity of each sample to temperature changes. By comparing D_0 and E_a values, the model highlights the unique diffusion potential and thermal resistance for each sample, offering a detailed understanding of how each material may respond to varying thermal environments based on its molecular structure or composition [40].

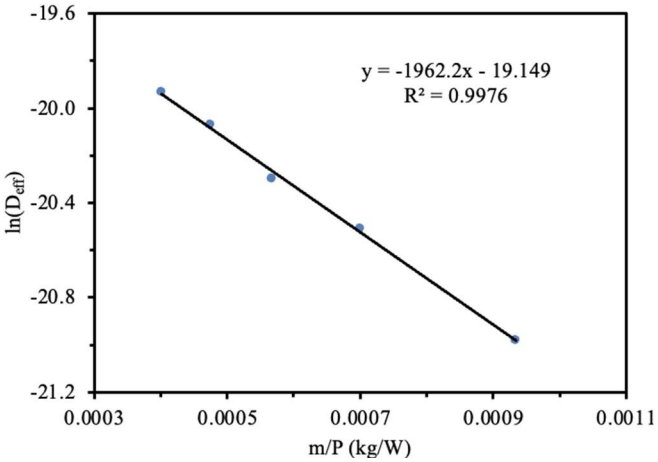

Figure 5. A relationship of the Arrhenius type between infrared power and effective moisture diffusivity.

When Eq. (15) is analysed, D_0 value is determined as 4.86×10^{-9} m²/s, and the E_a value is determined as 1.967 kW/kg. These results, with minor variations, align with earlier studies on the drying processes of black carrots

[28] and orange carrots [41]. These findings underscore the significant role of infrared power level and drying conditions in determining the activation energy necessary for moisture removal. The variability observed in activation energy during food drying processes is likely influenced by several factors, including the type of food, its moisture content, and the specific drying methods employed.

The E_a obtained in the present study (1.967 kW/kg) aligns with previously reported power-based values for carrots and carrot by-products. Doymaz [42] reported E_a = 4.247 kW/kg for carrot slices dried at 62–125 W using a modified Arrhenius approach, while E_a = 5.73 kW/kg was observed for carrot pomace (83–209 W) [43], and E_a = 3.65 kW/kg for black carrot pomace (104–230 W) [28]. The comparatively lower E_a reported here is justified by the use of lower IR power levels (38–88 W) and slightly thicker slices, which reduce power absorption per unit mass and shift drying toward a milder thermal regime.

Experimental factors such as slice thickness, sample mass, emitter-sample distance, initial moisture content, and the moisture range used for fitting D_{eff} substantially affect E_a determination. Toğrul [2] and Botelho *et al.* [32] emphasize that E_a should be interpreted within the context of these parameters, as lower IR powers generally result in slower drying rates and a smaller driving force, leading to reduced apparent E_a in power-based models.

This study contributes to the literature by providing new data on E_a behaviour under low-to-moderate IR power conditions—a regime that remains underexplored. The findings are particularly relevant for industrial applications aiming to optimize energy efficiency and minimize thermal damage while maintaining product quality.

Energy efficiency during the process of carrot drying

Energy efficiency values were calculated using Eq. (13), and Fig. 6 illustrates how energy efficiency varied over the drying period for infrared drying of yellow carrot slices. Energy efficiency was initially very high, reflecting greater infrared power absorption. As moisture content and energy absorption in the samples decreased, infrared power reflection increased instead. The highest energy efficiency was observed at an infrared power level of 88 W.

The energy efficiency of yellow carrot slices exhibited a considerable range, varying from 0.02% to 33.1%, corresponding to power levels between 38 W and 88 W, indicating a significant dependence of efficiency on applied power. These findings align with prior research conducted on okra [44], which reported analogous trends in energy efficiency under comparable power conditions, further substantiating the influence of power intensity on the energy conversion efficacy in vegetable processing. The observed variability underscores the need for optimizing power parameters to enhance efficiency in such applications.

CONCLUSION

This study systematically examined the drying behavior of carrot slices using an infrared dryer operated at power levels ranging from 38 to 88 W. The findings demonstrated that infrared radiation intensity exerted a significant influence on drying kinetics, particularly on drying time and effective moisture diffusivity. An increase in infrared power substantially reduced the overall drying duration by enhancing the moisture diffusion coefficient, which varied between 7.73×10^{-10} and 2.21×10^{-9} m²/s across the tested power range. All drying operations occurred within the falling-rate period, confirming that the moisture removal process was predominantly governed by internal diffusion mechanisms rather than surface evaporation. Among the mathematical models evaluated, the Midilli & Kucuk model exhibited the highest predictive accuracy, effectively characterizing the drying kinetics under various infrared power conditions.

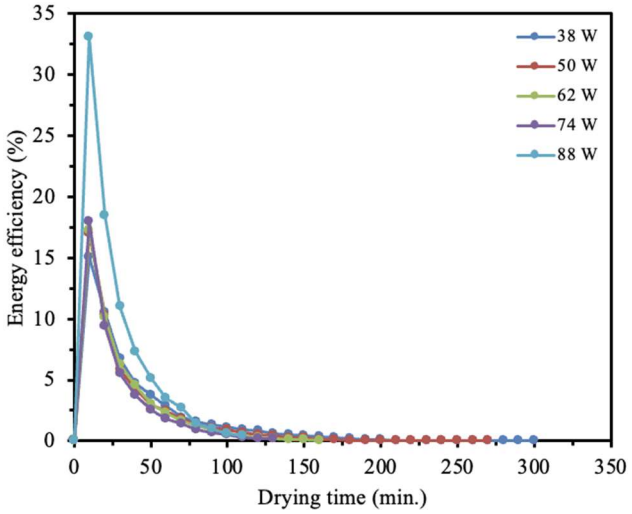

Figure 6. The change of energy efficiency (%) with respect to the infrared power level.

The activation energy, calculated using an Arrhenius-type relationship, was determined to be 1.967 kW/kg, representing the energy barrier for moisture diffusion. Although higher infrared power promoted accelerated moisture removal during the initial drying stages, prolonged exposure resulted in diminished energy efficiency due to the gradual reduction of the moisture gradient between the sample and the surrounding air, thereby lowering the driving force for mass transfer. These results emphasize the significance of defining infrared drying parameters through comprehensive kinetic modeling and energy performance evaluation rather than relying solely on process rate enhancement. The strong correlation between experimental data and the Midilli & Kucuk model underscores its applicability as a reliable predictive framework for process design and scale-up in infrared drying systems. Future investigations should integrate kinetic modeling with detailed energy analysis to further elucidate the relationship between power input, mass transfer behavior, and energy utilization efficiency, ultimately advancing the development of optimized, sustainable infrared drying technologies. Overall, the findings provide a valuable contribution to the understanding of infrared drying mechanisms, supporting the design of faster and more energy-efficient dehydration processes while maintaining desirable product characteristics.

LIST OF SYMBOLS

D_0: Pre-exponential factor in Arrhenius equation (m^2/s)
D_{eff}: Effective diffusivity (m^2/s)
E_a: Activation energy (W/kg)
K: Slope
L: Half the slice thickness of the sample
M: Moisture content (kg water/kg dry matter)
M_0: Initial moisture content (kg water/kg dry matter)
M_d: Dry weight (kg)
M_e: Equilibrium moisture content (kg water/kg dry)
MR_{exp}: Experimental moisture ratio
MR_{pre}: Predicted moisture ratio
M_t: Moisture content at any time (kg water/kg dry matter)
$M_{t+\Delta t}$: Moisture content at t+Δt
m_w: Mass of evaporated water (g)
M_W: Sample weight (kg)
n: Number of experimental data points
N: Number of parameters
P: Infrared power (W)
R^2: Coefficient of determination
Δt: Drying time (min.)
η: Drying efficiency
λ_w: Latent heat of vaporization
χ^2: Chi-square

ABBREVIATIONS

AOAC: Association of Official Agricultural Chemists
LDPE: Low-density polyethylene
MR: Moisture ratio
DR: Drying rate (kg water/kg dry matter * time)
RMSE: Estimated standard error
US: Ultrasound
HD: Hot air drying
MWD: Microwave drying
INFD: Infrared drying

REFERENCES

[1] A. Ignaczak, A. Salamon, J. Kowalska, A. Marzec, H. Kowalska, Molecules 28 (2023) 6407. https://doi.org/10.3390/molecules28176407.
[2] H. Toğrul, J. Food Eng. 77 (2006) 610-619. https://doi.org/10.1016/j.jfoodeng.2005.07.020.
[3] P. Sakare, N. Prasad, N. Thombare, R. Singh, S.C. Sharma, Food Eng. Rev. 12 (2020) 381-398. https://doi.org/10.1007/s12393-020-09237-w.
[4] N.K. Rastogi, Crit. Rev. Food Sci. Nutr. 52 (2012) 737-760. https://doi.org/10.1080/10408398.2010.508138.
[5] J.K. Yan, L.X. Wu, Z.R. Qiao, W.D. Cai, H. Ma, Food Chem. 271 (2019) 588-596. https://doi.org/10.1016/j.foodchem.2018.08.012.
[6] M. Younis, D. Abdelkarim, A. Zein El-Abdein, Saudi J. Biol. Sci. 25 (2018) 332-338. https://doi.org/10.1016/j.sjbs.2017.06.011.
[7] O.Y. Turan, F.E. Firatligil, Czech J. Food Sci. 37 (2019) 128-134. https://doi.org/10.17221/243/2017-CJFS.
[8] A. Solyom, J. Betz, P. Brown, A. Bzhelyansky, N. Chrisafis, M. Embuscado, H. Figore, H. Johnson, G. Joseph, D. Kennedy, A. Kuszak, E. Mudge, M. Phillips, T. Phillips, L. Richards, C. Rimmer, B. Sauza, B. Schaneberg, J. Skamarack, S. Coates, J. AOAC Int. 99 (2016) 1102-1104. https://doi.org/10.5740/jaoacint.SMPR2016.003.
[9] J. Akter, J. Hassan, M. M. Rahman, M. S. Biswas, H I. Khan, M.M.R. Rajib, M.R. Ahmed, M. N.-E.-A. Khan, M. F.A. Hasan, Heliyon 10 (2024) e24165. https://doi.org/10.1016/j.heliyon.2024.e24165.
[10] T. Gulati, A.K. Datta, J. Food Eng. 166 (2015) 119-138. https://doi.org/10.1016/j.jfoodeng.2015.05.031.
[11] P.C. Panchariya, Đ. Popović, A. Sharma, J. Food Eng. 52 (2002) 340-358. https://doi.org/10.1016/S0260-8774(01)00126-1.
[12] A. Manzoor, M.A. Khan, M.A. Mujeebu, R.A. Shiekh, J. Agric. Food Res. 5 (2021) 100176. https://doi.org/10.1016/j.jafr.2021.100176.
[13] D.C. Lopes, A.J. Steidle Neto, J.K. Santiago, Biosyst. Eng. 118 (2014) 105-114. https://doi.org/10.1016/j.biosystemseng.2013.11.011.
[14] A. Midilli, H. Kucuk, Energy Convers. Manage. 44 (2003) 1111-1122. https://doi.org/10.1016/S0196-8904(02)00099-7.
[15] A. Omolola, A. Jideani, P. Kapila, Interciencia 40 (2015) 374-380. https://www.researchgate.net/publication/282237695_Drying_kinetics_of_banana_Musa_spp.
[16] M. Aghbashlo, M. Kianmehr, S. Khani, M. Ghasemi, Int. Agrophys. 23 (2009) 313-317. http://www.international-agrophysics.org/Mathematical-modelling-of-thin-layer-drying-of-carrot,106450,0,2.html#ungrouped
[17] M.M.M. Najla, R. Bawatharani, Iconic Res. Eng. J. 2 (2019) 6-10. https://www.irejournals.com/paper-details/1701096.
[18] S. Shah, M. Joshi, Int. J. Electron. Eng. 2 (2010) 159-163. https://www.semanticscholar.org/paper/Modeling-Microwave-Drying-Kinetics-of-Sugarcane-Shah-Joshi/e0b913d263f9f955b27e4eac3aa323be2e676089.
[19] S. Jena, H. Das, J. Food Eng. 79 (2007) 92-99. https://doi.org/10.1016/j.jfoodeng.2006.01.032.
[20] R. Lemus-Mondaca, N. Betoret, A. Vega-Gálvez, E. Lara-Aravena, J. Food Process Eng. 32 (2009) 645-663. https://doi.org/10.1111/j.1745-4530.2007.00236.x.
[21] R. Guiné, Electron. J. Environ. Agric. Food Chem. 9 (2010) 1772-1783. https://www.researchgate.net/publication/256444660_Analysis_of_the_drying_kinetics_of_S_Bartolomeu_pears_for_different_drying_systems.
[22] B. Alaei, R. Chayjan, J. Food Process. Preserv. 39 (2014) 1-12. https://doi.org/10.1111/jfpp.12252.
[23] T.J. Afolabi, T.Y. Tunde-Akintunde, J.A. Adeyanju, J. Food Sci. Technol. 52 (2015) 2731-2740. https://doi.org/10.1007/s13197-014-1365-z.
[24] L. Hassini, S. Azzouz, R. Peczalski, A. Belghith, J. Food Eng. 79 (2007) 47-56. https://doi.org/10.1016/j.jfoodeng.2006.01.025.

[25] J. Crank, The Mathematics of Diffusion, 2nd ed., Oxford University Press, London (1975), p. 69-88. https://dokumen.pub/the-mathematics-of-diffusion-second-edition-0198533446-9780198533443.html.
[26] N.P. Zogzas, Z.B. Maroulis, Dry. Technol. 14 (1996) 1543-1573. https://doi.org/10.1080/07373939608917163.
[27] L. Ceclu, E. Botez, O. Nistor, F. Gögüs, D. Andronoiu, G. Mocanu, Ann. Univ. Dunarea Jos Galati 39 (2015) 20-29. https://www.researchgate.net/publication/298842746_Influence_of_drying_conditions_on_the_effective_diffusivity_and_activation_energy_during_convective_air_and_vacuum_drying_of_pumpkin.
[28] İ. Doymaz, Sigma J. Eng. Nat. Sci. 37 (2019) 71-84. https://dergipark.org.tr/en/pub/sigma/issue/65450/1011078#article_cite.
[29] J. Yi, X. Li, J. He, X. Duan, Dry. Technol. 38 (2019) 1-16. https://doi.org/10.1080/07373937.2019.1628772.
[30] D. Huang, P. Yang, X. Tang, L. Luo, B. Sunden, Trends Food Sci. Technol. 110 (2021) 765-777. https://doi.org/10.1016/j.tifs.2021.02.039.
[31] M. Zarein, S.H. Samadi, B. Ghobadian, J. Saudi Soc. Agric. Sci. 14 (2015) 41-47. https://doi.org/10.1016/j.jssas.2013.06.002.
[32] F. Botelho, P. Correa, A. Goneli, M. Martins, F. Magalhães, S. Campos Botelho, Rev. Bras. Eng. Agric. Ambient. 15 (2011) 845-852. https://doi.org/10.1590/S1415-43662011000800012.
[33] H. Elmesiry, K. Ashiagbor, Z. Hu, W.G. Alshaer, Case Stud. Therm. Eng. 52 (2023) 103676. https://doi.org/10.1016/j.csite.2023.103676.
[34] A.M. Matouk, M.M. El-Kholy, A. Tharwat, W.M. Abdelrahman, J. Soil Sci. Agric. Eng. 5 (2014) 569-581. https://doi.org/10.21608/jssae.2014.49310.
[35] B. Turkan, A.B. Etemoglu, Sigma J. Eng. Nat. Sci. 38 (2020) 527-544. https://dergipark.org.tr/en/pub/sigma/issue/65153/1002263.
[36] S. Álvarez, C. Álvarez, R. Hamill, A.M. Mullen, E. O'Neill, Compr. Rev. Food Sci. Food Saf. 20 (2021) 5370-5392. https://doi.org/10.1111/1541-4337.12845.
[37] R. Shrestha, A. Dhungel, S. Dhakal, Tribhuvan Univ. J. Food Sci. Technol. 2 (2023) 17-25. https://doi.org/10.3126/tujfst.v2i2.66508.
[38] M.Y. Barforoosh, A.M. Borghaee, S. Rafiee, S. Minaei, B. Beheshti, Int. J. Low-Carbon Technol. 19 (2024) 192-206. https://doi.org/10.1093/ijlct/ctad121.
[39] H.S. El-Mesery, M. Qenawy, Z. Hu, W.G. Alshaer, Case Stud. Therm. Eng. 50 (2023) 103451. https://doi.org/10.1016/j.csite.2023.103451.
[40] F. Yang, H. Schmidt, E. Hüger, ACS Omega 8 (2023) 27776-27783. https://doi.org/10.1021/acsomega.3c04029.
[41] İ. Doymaz, J. Food Process. Preserv. 39 (2015) 2738-2745. https://doi.org/10.1111/jfpp.12524.
[42] İ. Doymaz, J. Agric. Sci. 19 (2013) 1-11. https://doi.org/10.1501/Tarimbil 0000001227.
İ. Doymaz, Sigma J. Eng. Nat. Sci. 37 (2019) 161-171.https://dergipark.org.tr/en/pub/sigma/issue/65450/1011078.
[43] S. Tanta, İ. Doymaz, Sigma J. Eng. Nat. Sci. 37 (2019) 93-104. https://dergipark.org.tr/en/pub/sigma/issue/65450/1011084.

MEHMET SOYDAN

İBRAHIM DOYMAZ

Yildiz Technical University, Department of Chemical Engineering, 34220 Esenler, İstanbul, Türkiye

INFRACRVENO SUŠENJE KRIŠKI ŠARGAREPE: UTICAJ NIVOA SNAGE NA KINETIKU I ENERGETSKU EFIKASNOST

Cilj ove studije je optimizacija uslova sušenja žute šargarepe istraživanjem efekata različitih nivoa snage infracrvenog (IC) zračenja na kinetiku sušenja. Nakon testova sušenja na nivoima snage IC zračenja od 38, 50, 62, 74 i 88 W, početni sadržaj vlage u kriškama šargarepe (6,95 kg vode/kg suve materije) smanjen je na 0,11 kg vode/kg suve materije. Vremena sušenja kretala su se od 300 minuta pri 38 W do 110 minuta pri 88 W, što pokazuje obrnutu vezu između snage IC zračenja i trajanja sušenja. Viši nivoi snage IC zračenja ubrzali su sušenje poboljšanjem prenosa energije, što je podstaklo efikasnost uklanjanja vlage. Efektivni koeficijenti difuzije, izračunati u rasponu od $7,73\times10^{-10}$ do $2,21\times10^{-9}$ m²/s za nivoe snage od 38 W do 88 W, ukazuju na povećanje migracije vlage sa većom snagom. Energetske potrebe procesa odražene su u energiji aktivacije za difuziju vlage (1,967 kW/kg). Model Midilija i Kučuka ponudio je najbolje rešenje za karakterizaciju ponašanja sušenja, a statistička analiza je potvrdila ispravnost modela. Ovi nalazi pružaju vredne uvide za optimizaciju uslova infracrvenog sušenja kako bi se poboljšala efikasnost i kvalitet procesa sušenja žute šargarepe.

Ključne reči: Infracrveno sušenje, matematičko modelovanje, kinetika sušenja, koeficijent difuzije, energija aktivacije.

NAUČNI RAD